

Lawrence Berkeley National Laboratory

Recent Work

Title

Calculation of Cross Sections for Binary Reactions between Heavy Ion Projectiles and Heavy Actinide Targets

Permalink

<https://escholarship.org/uc/item/3k13w21n>

Authors

Hoffman, D.C.
Hoffman, M.M.

Publication Date

1990-11-01



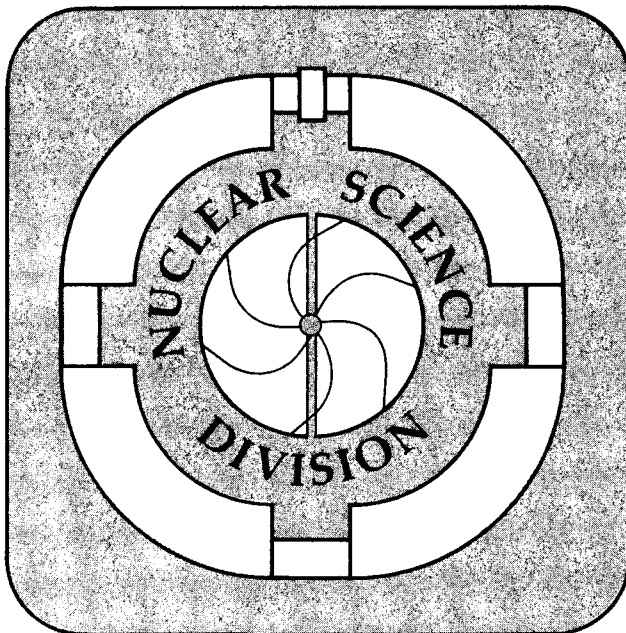
Lawrence Berkeley Laboratory

UNIVERSITY OF CALIFORNIA

Calculation of Cross Sections for Binary Reactions between Heavy Ion Projectiles and Heavy Actinide Targets

D.C. Hoffman and M.M. Hoffman

November 1990



For Reference

Not to be taken from this room

DISCLAIMER

This document was prepared as an account of work sponsored by the United States Government. While this document is believed to contain correct information, neither the United States Government nor any agency thereof, nor the Regents of the University of California, nor any of their employees, makes any warranty, express or implied, or assumes any legal responsibility for the accuracy, completeness, or usefulness of any information, apparatus, product, or process disclosed, or represents that its use would not infringe privately owned rights. Reference herein to any specific commercial product, process, or service by its trade name, trademark, manufacturer, or otherwise, does not necessarily constitute or imply its endorsement, recommendation, or favoring by the United States Government or any agency thereof, or the Regents of the University of California. The views and opinions of authors expressed herein do not necessarily state or reflect those of the United States Government or any agency thereof or the Regents of the University of California.

LBL-29502

CALCULATION OF CROSS SECTIONS FOR BINARY REACTIONS
BETWEEN HEAVY ION PROJECTILES AND HEAVY ACTINIDE TARGETS

Darleane C. Hoffman

*Department of Chemistry
University of California, Berkeley
and Nuclear Science Division
MS-70A/3307, Lawrence Berkeley Laboratory
1 Cyclotron Road
Berkeley, CA 94720*

and

Marvin M. Hoffman

November, 1990

This work supported in part by the Director, Office of Energy Research, Office of Nuclear Physics of the Office of High Energy and Nuclear Physics of the U. S. Department of Energy under Contract DE-AC03-76SF00098.

INTRODUCTION

Radiochemical analyses have provided cross section values¹⁻⁸ for the production of specific nuclei in heavy ion reactions with heavy actinide targets such as ²⁴⁸Cm, ²⁴⁹Cf, and ²⁵⁴Es. Data from heavy ion experiments in which actinide target nuclei are bombarded by projectiles with kinetic energies very near the nuclear Coulomb barrier show that nuclei with mass and charge close to the values of the target nuclei are formed with large cross sections, of the order of thousands of microbarns. These large production cross sections lead to the conclusion that the heavy products are formed from binary transfer reactions rather than from compound nucleus formation. De-excitation of a compound nucleus via the emission of many particles and the consequent severe depletion via fission at each step would be expected to result in very small cross sections. Based on a simple binary transfer mechanism, we showed earlier⁹ that many of the reactions producing neutron-rich target-like products have rather small Q values. Thus the residual heavy products have low excitation energies, and the probability for losses due to prompt fission and particle emission are greatly reduced compared to products produced by complete fusion with resultant large excitation energies and subsequent particle emission or fission. Previous heavy ion experiments have shown that the cross section for formation of a specific product nucleus depends strongly on the total number of nucleons transferred. Differences in the mass surface, i.e., the ground state Q values for the reactions, also strongly affect the cross section. In our previous report⁹, we tabulated the calculated excitation energies for transcurium products up to Z=103 (later extended to below target products with Z=92 to 96) for binary reactions between ¹⁶O, ¹⁸O, ²⁰Ne, and ²²Ne projectiles and ²⁴⁵Cm, ²⁴⁶Cm, ²⁴⁸Cm, ²⁴⁹Cf, and ²⁵²Cf targets, and for ¹²C and ⁴⁸Ca projectiles with ²⁵⁴Es and ²⁵⁷Fm targets. Projectile energies approximately equal to the calculated Coulomb barriers were considered. For higher projectile energies, the excess kinetic energy was apportioned between the products according to the fraction of the projectile mass transferred to the heavy product.

The computer program, described here, is identified as PWAVED5. It was developed

to calculate cross sections for nucleon transfer reactions in low energy heavy ion bombardments. The objective was to calculate cross sections that agree with experimental results for ions of different charge and mass and to develop a predictive capability. It was undertaken because previous heavy ion calculations, for which programs were readily available, appeared to focus primarily on reactions resulting in compound nucleus formation and were not particularly applicable to calculations of binary reaction cross sections at low interaction energies.

There are two principal areas in which this computation differs from several other partial wave calculations of heavy-ion reaction cross sections. First, this program is designed specifically to calculate cross sections for nucleon exchange interactions and to exclude interactions that are expected to result in fusion of the two nuclei. A second major difference in this calculation is the use of a statistical distribution to assign the total interaction cross section to individual final mass states.

Ion trajectories are designed to limit the calculated cross sections to binary exchange interactions. It is assumed that in near-grazing collisions nuclei will scatter and exchange nucleons but will not fuse. If the collision is energetic enough to distort and drive the nuclei together significantly, the interaction will result in fusion. To eliminate fusion events from the calculated cross section, only trajectories having radial kinetic energies in a small interval above the Coulomb barrier are allowed.

The desired trajectories are selected by using the Rutherford formula to find the point of closest approach of the two ions. The distance of closest approach corresponds to radial kinetic energy in this formula. By selecting an appropriate range for the closest approach, the desired range of radial kinetic energies is selected.

Specifically, the distance of closest approach must be equal to or less than the sum of the projectile and target radii, R_1+R_2 , and greater than the distance between the centers of these nuclei when they are in a position which simulates the fission saddle point configuration. In this problem, a distance of $R_2+(0.6)R_1$ between the nuclear centers has been used to repre-

sent the saddle point separation.

Experiments show that heavy ion bombardment of massive target nuclei at energies near the Coulomb barrier can result in the exchange of nucleons when the reaction is energetically allowed. Experimental conditions indicate that only a brief contact between the nuclei is necessary for the exchange of many nucleons. The observation that one, two, or more, up to as many as eleven nucleons may be exchanged with different probabilities indicates that the nucleon transfer can be represented by a statistical process. In the current computation, the calculated geometric cross section is distributed among the transfer of 1 to 12 nucleons with the Gaussian probability centered on a mean value proportional to the amount of nuclear overlap for each case.

Cross sections were calculated for products with Z larger than that of the target assuming a binary transfer reaction mechanism. Yields for the heavy products as a function of the number of nucleons transferred and as a function of the kinetic energy of the projectile are given. The calculation also includes the effects of nuclear kinematics due to changes in the mass and charge of projectiles and targets.

CALCULATIONAL METHODS

Total Cross Section for Binary Reactions

The starting point for this problem was a calculation of the geometric cross section for interaction between projectiles and target atoms. This was calculated from the classical hyperbolic, i.e., positive-energy, solution for the repulsive inverse-square force problem. Equations applicable to the two-body repulsive central force problem are given in Appendix A. Coulomb forces alone determine the relative motion of projectile and target nuclei in this solution so the resulting trajectories are accurate only until the nuclei first make contact and short range nuclear forces become important.

The general solution for the orbit of a particle about a fixed point for a repulsive

Coulomb force is given by: $1/r = (mzz')/(e/L)^2(1 + \epsilon \cos\theta)$, where $\epsilon^2 = 1 + (2Es/zz'e^2)^2$. If only central forces act in a two body system, the orbit lies in a plane so only two coordinates, (r) and (θ) , are required to define the motion. In a conservative system there are two constants of motion, the total energy (E) and the angular momentum (L) . The reduced mass of the system is represented by (m) ; z and z' are the nuclear charges and s is the impact parameter of the incoming ion. Orbits of central force problems represent conic sections with one focus at the scattering point. The parameter (ϵ) defines the nature of the orbit. This problem is concerned only with systems having total energy greater than zero, corresponding to $\epsilon > 1$, which leads to hyperbolic trajectories for the Rutherford orbits. The simple form of the orbit equation given above requires that the center of force be located at the origin of the coordinate system and that the $\theta = 0$ and 180° axis must pass through the foci of the hyperbola. Under these conditions the value of $\cos\theta$ must be negative so θ will always be in the second and third quadrants and be symmetric about 180° . (Some details of the solution used here are given in Appendix A of this report. For a complete treatment, see Goldstein¹⁰, Chapter 3.)

Our program solves the equation of Rutherford orbits for selected values of the fixed parameters E , m , z and z' , and for a range of values of the impact parameter s . The impact parameter correlates directly with the system angular momentum, L , and with the distance of closest approach, corresponding to $\cos\theta = -1$ in the orbit equation. The calculated value of closest approach is not accurate if it is less than the sum of the two ionic radii because of nuclear forces which disturb the orbit. Extending the calculation into the region of nuclear overlap, while not representing accurate configurations, does, however, provide a good measure of the radial kinetic energy of the ions at their point of contact.

The concept of two nuclei moving together along their line of centers is useful in establishing limits of integration on geometric cross sections which represent binary reactions between heavy ions. Specifically, if motion along the (r) coordinate is stopped by Coulomb repulsion prior to the nuclei coming into contact, no interaction occurs because the relative

kinetic energy is below the Coulomb barrier. If the turning point comes just as the nuclei make contact, the energy is at the barrier and the grazing trajectory results; if the nuclei come into contact while they are still moving together with excess kinetic energy they will be forced together in a configuration which, to some extent, will resemble a fission saddle point configuration. If motion along this axis goes beyond this saddle point the two nuclei would be expected to fuse into a compound nucleus. Thus, trajectories which bring the two ions into contact, but not into the saddle point configuration, are expected to result in binary reactions.

Two adjustable parameters, CD and RD , (see Appendix A, Eqs. 11 and 12) were used to designate the trajectories which we have defined to result in binary interactions. For $RD < 0$ the ions do not make contact so no interaction is possible. At $RD = 0$ the distance of closest approach is equal to the sum of the two nuclear radii representing a grazing trajectory. For trajectories with $RD > 0$, the two ions come into contact and binary reactions can occur. The second parameter, CD , is used to establish a point which separates the region in which binary reactions are expected from that in which fusion of the two ions is predicted. Thus, trajectories for which $CD > 0$ lead to fusion and make no contribution to the binary cross section; if $CD < 0$ and $RD > 0$ the interaction results in a binary exchange of nucleons.

For any set of input parameters the program will find the impact parameters and the corresponding angular momenta for which $RD = 0$ and $CD = 0$. Integration of the impact parameter area within these limits results in the desired geometric cross section and the corresponding angular momenta are used as the limits of summation in the partial wave calculation. Comparing cross section values derived by these two methods reveals the effect of angular momentum quantization which can be significant for interactions very near the Coulomb barrier. Appendix B lists all variables and constants used in the computer program. Appendix C gives a listing of the program, and Appendix D shows the complete flow diagram.

Nucleons Transferred

Heavy ion trajectories that satisfy the criteria, $CD < 0 < RD$, will result in physical contact

between the two nuclei for times usually not in excess of 2.0×10^{-21} s. This is ample time for the exchange of several nucleons. It is assumed that during the interaction, nucleons can move either from projectile to target or in the reverse direction with statistically defined probabilities. It was further assumed that the most probable number of nucleons exchanged would be correlated with the volume of the nuclear overlap region and that the exchange of greater or lesser numbers would be represented by a normal (Gaussian) distribution about the most probable value. The standard deviation of the Gaussian is an adjustable parameter.

Program lines 1110 through 1150 estimate the most probable number of nucleons exchanged and lines 1305 through 1345 assign the total cross section for binary interactions among twelve different mass numbers according to the Gaussian distribution. These program steps are repeated for each incremental step in the impact parameter over the interval $CD < 0 < RD$. The current program sums only nucleon transfers from projectile to target although transfers in the other direction could also be recorded if it were desirable.

If the full printout option is used by setting the flag $NPRT = 0$, the contribution to the cross section for each mass number from each iteration and also the cumulated sum are printed on the line printer. The abbreviated printout (for $NPRT = 1$) gives only the final iteration and cumulated sum. All output is displayed on the screen for either print option.

Transmission Factors

The transfer of nucleons between interacting ions is expected to be strongly influenced by the final state energies of the resulting nuclei. These effects can be introduced by multiplicative transmission functions applied to the geometric cross sections. Currently all transmission functions are set to one so the calculational results are purely geometrical.

CALCULATIONAL RESULTS

Output

The output of this calculation is tabulated as the cross section for the net transfer of (x)

nucleons from projectile to target, or vice versa, without regard for whether they are neutrons or protons. The same will generally not be true of the experimental results with which the calculation is compared. The radiochemical yield experiments measure cross sections for the net effective transfer of (x) nucleons, of which a specific number, p , are protons and a specific number, n , are neutrons. For the target-like product, $x = |±p| + |±n|$. The radiochemical data for the target-like product yields may be compared with the results of the calculation if provision is made for the fact that a specific number of both neutrons and protons must be transferred, either to or from the target, not just a total number of nucleons. For a system with equal numbers of protons and neutrons, the multiplicity is $4x$. In lines 1331 and 1332 of the code, provision is made for a correction of $4x$ for multiplicity. Whether or not this correction is implemented is determined by the decision flag, VVV (see Appendix B). It should be emphasized that this correction is based on the assumption of equal numbers of neutrons and protons and that the probability for their transfer is identical.

COMPARISON WITH DATA

Multiplicity Corrections

The measured cross sections for above target actinides from the reactions of ^{248}Cm and ^{18}O and ^{16}O projectiles are given in Tables I and II and plotted in Figures 1 and 2. These have been taken from Lee et al.^{1,2}; cross sections have been included only for those heavy products whose excitation energy, E^* , calculated as in our earlier paper⁹, is in the range from about 0 to 10 MeV. The measured cross section value for a given isotope represents only 1 of $4x$ ways of transferring x nucleons if the probability of transferring a proton, p_p , equals the probability of transferring a neutron, p_n , = 0.5. This correction can be made in the code as discussed earlier. However, for different probabilities for the transfer of neutrons and protons, it seemed more convenient to correct the experimental data, rather than the calculation, for different values of these probabilities based on the fraction of protons in the system of interest. For example, the

production of ^{253}Cf involves the net effective transfer of 2 protons and 3 neutrons from the projectile to the ^{248}Cm target; therefore, $x = |+2| + |+3| = 5$, and the number of ways to transfer 5 nucleons is $4x$ or 20. The experimental cross section for ^{253}Cf must then be multiplied by 20 before comparison with the calculation which includes all possible ways to transfer 5 nucleons. For ^{247}Cf , 2 protons must be transferred to the target and 3 neutrons to the projectile; again, $x = |+2| + |-3| = 5$. However, since these systems have more neutrons than protons, it seems reasonable that the neutron transfer probability should be larger than that for protons, but it is not obvious what the appropriate value should be as it is not clear what the neutron-to-proton ratio may be in the overlap volume. Therefore, the limiting cases of the composition of the target where $p/(p+n) = 0.613$ and $n/(p+n) = 0.387$, and of ^{16}O which has equal numbers of protons and neutrons were considered. The probability for transferring a proton (or neutron) was taken as equal to its fraction of the total number of nucleons. The probabilities for a given number of protons transferred out of a total of x nucleons transferred were then calculated for each heavy product using the binomial theorem: $P(p) = x! / [(x-p)! p!]^{-1} p_p^p (1-p_p)^{x-p}$.

For the totally equilibrated compound system, $^{248}\text{Cm} + ^{16}\text{O}$, $p_p = 0.394$, obviously very close to the target composition. The experimental cross sections, and the values after correction for multiplicity using $p_p = 0.500$ and $p_p = 0.387$, are listed in Tables I and II. These data are also plotted, together with solid lines representing the calculated cross sections which give the best fit to the experimental data, in Figures 3.(a) and (b) and 4.(a) and (b) as a function of x , the total number of nucleons transferred.

Gaussian Distributions

The transfer cross sections calculated for $^{248}\text{Cm} + ^{18}\text{O}$ at an energy 1.4 MeV above the Coulomb barrier for Gaussian distributions with standard deviation, σ , of 1.6, 1.8, and 2.0 are plotted in Figure 5. A similar plot for interactions with ^{16}O is given in Figure 6. The calculation with $\sigma = 1.8$ for a projectile energy between 1.4 MeV and 3.3 MeV above the barrier seems to give the best fit to the ^{18}O data which has been corrected for multiplicity based on

either $p_p = 0.39$ (the fraction of protons in ^{248}Cm) or $p_p = 0.5$. The calculation with $\sigma = 1.6$ appears to be slightly better for the ^{16}O system, although the scatter in the data is so large that it is difficult to tell.

Energy Dependence

Figures 7 and 8 show the changes in calculated cross sections as a function of projectile energy above the Coulomb barrier. As expected, the calculated cross sections increase with energy, but the experimental values will, of course, ultimately decrease as the fission barriers (around 5.5 MeV) or neutron binding energies are exceeded. This effect has not yet been incorporated in the calculations and, therefore, only experimental cross sections with calculated excitation energies, E^* , which are positive but less than about 10 MeV above the reaction barrier are used in the comparisons with the calculations. Based on the energy at which the experimental cross sections decreased as a function of projectile energy, Lee et al.² have observed that only about 0.6 of the excess projectile energy appears as excitation energy of the target-like product in interactions of ^{18}O with ^{248}Cm .

DISCUSSION

After correction of the experimental cross sections for multiplicity, the results of the PWAVED5 calculation reproduce the general features of the experimental data rather well. In principle, it should be possible to determine from the experimental data whether the value of p_p for the target or projectile gives a better fit and thus infer whether the composition of the overlap volume is more representative of the target (or compound system) or of the projectile. However, the scatter in the experimental data does not permit this kind of detailed comparison.

Another question of primary interest is whether the calculation is applicable to other systems of this type. In order to check this, as well as its predictive capability, we have done similar calculations for ^{249}Cf and ^{254}Es with ^{16}O and ^{18}O and compared them with the experi-

mental data for these systems. The experimental data for ^{254}Es reactions with ^{18}O , corrected for multiplicity, are shown in Fig. 9 together with lines representing the cross sections calculated at 1.4 MeV above the Coulomb barrier for both $\sigma = 1.6$ and 1.8. The fit appears to be somewhat better for 1.6. It should be noted that the calculated cross section for a given number of nucleons transferred is about the same for these targets as for ^{248}Cm . Thus, for energetically favorable reactions, use of a neutron-rich target enhances the yield of neutron-rich heavy products. In addition, due to large differences in the binding energies of the complementary $Z=1$ to 4 products from ^{16}O and ^{18}O reactions, use of ^{18}O projectiles gives maxima in the isotopic distributions for the products with up to 4 Z greater than the target which are about two mass units heavier than for ^{16}O projectiles.

Currently, the experimental data are not sufficiently accurate nor extensive to permit stringent testing of the predictive capability of the model. For example, data for nucleon transfers of more than 8 nucleons are nearly non-existent and the point for 11 nucleons transferred shown in Fig. 3 is only an estimate. Such information is crucial in determining whether the rather rapid decrease in calculation predicted by the calculation is reasonable. If the point at $x = 11$ is considered, the experimental data shown in Fig. 1 would be better fit with a simple exponential function.

The calculated change in geometric cross section for the entire range of actinide targets is quite small as expected. However, the geometric cross sections vary considerably for the wide wide range of mass and charge of available projectiles. For example, the geometric cross sections differ by more than a factor of two for oxygen and calcium projectiles with energies near the Coulomb barrier. Nevertheless, the change is difficult to confirm experimentally because of the dominant, but inaccurately known, effect of the differing Q -values for the relevant reactions.

Reaction cross sections as a function of projectile energy have been measured for many different heavy ion reactions. Again, the interpretation of these data is complicated by incom-

plete information on the reaction energies. The current calculation predicts a linear increase in cross section as the projectile energy is increased over the Coulomb barrier. The increase in cross section continues until the critical energy is reached. For projectile energies above the critical energy the geometric cross section remains approximately constant. Reaction cross sections as a function of projectile energy have been measured for many different heavy ion reactions, but interpretation of the data is complicated by the reaction energies of the various nucleon transfer reactions.

Because of the absence of information on the reaction energy available for the different nucleon transfer channels and the strong influence of reaction energy on the nucleon transfer cross sections, it can only be noted that the available data do not contradict the predicted relationship between geometric cross section and energy in this calculation. Much additional data for larger nucleon transfers and for a variety of other systems will be essential in assessing the general applicability of the calculation.

TABLE I. Experimental Cross Sections for $^{248}\text{Cm} + ^{18}\text{O}$ and Values Corrected for Multiplicity with $p_p = 0.5$ and 0.39 .
(Experimental cross sections taken from Refs. 1 and 2.)

Nuclide	x	E^* (MeV)	Cross Section (μb)	Corrected Cross Sections	
				$p_p = 0.50$	$p_p = 0.39$
Bk-250	2	-2.5	1970	15800	16500
Cf-250	2	1.8	1300	10400	17100
Bk-251	3	1.2	>420	>4500	>3850
Cf-252	4	6.9	337	3590	3960
Cf-253	5	3.2	49	310	570
Es-253	5	1.0	29	185	520
Cf-254	6	3.9	3.3	28	41
Es-254	6	0.8	9.2	59	140
Fm-254	6	0.4	3.1	27	95
Es-255	7	3.2	0.31	4.6	4.3
Fm-255	7	2.3	1.1	16.	24.
Fm-256	8	8.2	0.33	4.9	5.9
Fm-259	11	-3.7	$\sim 0.01^a$	~ 0.3	~ 0.2

^aEstimated from Hoffman et al., Ref. 11.

TABLE II. Experimental Cross Sections for $^{248}\text{Cm} + ^{16}\text{O}$ and Values Corrected for Multiplicity with $p_p = 0.5$ and 0.39 .
(Experimental cross sections taken from Ref. 1.)

Nuclide	x	E^* (MeV)	Cross Section (μb)	Corrected Cross Sections	
				$p_p=0.50$	$p_p=0.39$
Bk-248m	2	-1.1	1600	12800	13450
Cf-250	2	8.6	1100	8800	14500
Cf-249	3	3.6	1700	18100	24300
Es-251	3	2.3	38	610	1270
Bk-246	4	-4.1	81	1300	920
Cf-248	4	2.6	500	5300	5880
Cf-252	4	6.0	4.3	46	51
Es-252	4	2.4	21	330	580
Fm-252	4	2.4	3.5	110	310
Bk-245	5	-3.4	11.	140	160
Es-253	5	5.0	7.4	47	130
Fm-251	5	-6.3	4.9	63	275
Fm-253	5	4.5	3.9	50	220
Cf-246	6	-5.4	6.2	53	79
Fm-254	6	10.1	1.3	11	41
Fm-255	7	8.1	0.3	4.4	6.5
Fm-256	8	12.5	0.02	0.3	0.35
Md-256	8	5.6	0.005	0.09	0.17

REFERENCES

1. D. Lee, H. von Gunten, B. Jacak, M. Nurmia, Y.-f. Liu, C. Luo, T. T. Seaborg, and D. C. Hoffman, *Phys. Rev. C* 25, 286 (1982).
2. D. Lee, K. J. Moody, M. J. Nurmia, G. T. Seaborg, H. R. von Gunten, and D. C. Hoffman, *Phys. Rev. C* 27, 2656 (1983).
3. R. L. Hahn, P. F. Dittner, K. S. Toth, and O. L. Keller, *Phys. Rev. C* 10, 1889 (1974).
4. A. G. Demin, V. A. Druin, Y. V. Lobanov, R. N. Sagaidak, V. K. Ultenkov, and S. Hübener, *Internatl. Symp. Synthesis and Properties of New Elements, Dubna, 1980, Abstracts D7-80-556*, p. 60.
5. D. C. Hoffman, M. M. Fowler, W. R. Daniels, H. R. von Gunten, D. Lee, K. J. Moody, K. Gregorich, R. Welch, G. T. Seaborg, W. Brüchle, M. Brügger, H. Gäggeler, M. Schädel, K. Sümmerer, G. Wirth, Th. Blaich, G. Herrmann, N. Hildebrand, J. V. Kratz, M. Lerch, and N. Trautmann, *Phys. Rev. C* 31, 1763 (1985).
6. H. Gäggeler, W. Brüchle, M. Brügger, M. Schädel, K. Sümmerer, G. Wirth, J. V. Kratz, M. Lerch, Th. Blaich, G. Herrmann, N. Hildebrand, N. Trautmann, D. Lee, K. J. Moody, K. E. Gregorich, R. B. Welch, G. T. Seaborg, D. C. Hoffman, W. R. Daniels, M. M. Fowler, H. R. von Gunten, *Phys. Rev. C* 33, 1983 (1986).
7. M. Schädel, W. Brüchle, M. Brügger, H. Gäggeler, K. J. Moody, D. Schardt, K. Sümmerer, E. K. Hulet, A. D. Dougan, R. J. Dougan, J. H. Landrum, R. W. Lougheed, J. F. Wild, and G. D. O'Kelley, *Phys. Rev. C* 33, 1547 (1986).
8. R. C. Chasteler, R. A. Henderson, D. Lee, K. E. Gregorich, M. J. Nurmia, R. B. Welch, and D. C. Hoffman, *Phys. Rev. C* 36, 1820 (1987).
9. Darleane C. Hoffman and Marvin M. Hoffman, "Calculated Excitation Energies for Transcurium Products of Binary Heavy Ion Reaction", Los Alamos National Laboratory Report LA-UR-82-824; revised, 1984.
10. Herbert Goldstein, *Classical Mechanics*, Addison-Wesley Press, Inc., Cambridge, Massachusetts, 1950.
11. D. C. Hoffman, D. Lee, A. Ghiorso, M. J. Nurmia, K. Aleklett, and M. Leino, *Phys. Rev. C* 24, 495 (1981).

FIGURE CAPTIONS

Figure 1. Experimental data for $^{248}\text{Cm} + ^{18}\text{O}$.

Figure 2. Experimental data for $^{248}\text{Cm} + ^{16}\text{O}$.

Figure 3. (a) Experimental data for $^{248}\text{Cm} + ^{18}\text{O}$ corrected for multiplicity. Solid symbols are for $p_p = 0.39$ and open symbols are for 0.50.

(b) The solid line represents the cross sections calculated for $B + 1.4$ MeV and $\sigma = 1.8$.

Figure 4. (a) Experimental data for $^{248}\text{Cm} + ^{16}\text{O}$ corrected for multiplicity. Solid symbols are for $p_p = 0.39$ and open symbols are for 0.50.

(b) The solid line represents the cross sections calculated for $B + 1.4$ MeV and $\sigma = 1.6$.

Figure 5. Calculated cross sections for $^{248}\text{Cm} + ^{18}\text{O}$ at a projectile energy 1.4 MeV above the Coulomb barrier ($B + 1.4$ MeV) for Gaussian distributions with $\sigma = 1.6, 1.8,$ and 2.0.

Figure 6. Calculated cross sections for $^{248}\text{Cm} + ^{16}\text{O}$ at $B + 1.4$ MeV for Gaussian distributions with $\sigma = 1.6, 1.8,$ and 2.0.

Figure 7. Calculated cross sections for $^{248}\text{Cm} + ^{18}\text{O}$ for $\sigma = 1.8$ and $B + 1.4, 3.3,$ and 5.2 MeV.

Figure 8. Calculated cross sections for $^{248}\text{Cm} + ^{16}\text{O}$ for $\sigma = 1.6$ and $B + 1.4, 2.4, 3.0,$ and 4.9 MeV.

Figure 9. Experimental data for $^{254}\text{Es} + ^{18}\text{O}$ corrected for multiplicity. Solid symbols are for $p_p = 0.39$ and open symbols are for 0.50. Calculated cross sections for $B + 1.4$ MeV for Gaussian distributions with $\sigma = 1.6$ and 1.8 are shown for comparison.

$^{248}\text{Cm} + ^{18}\text{O}$
(EXPERIMENTAL)

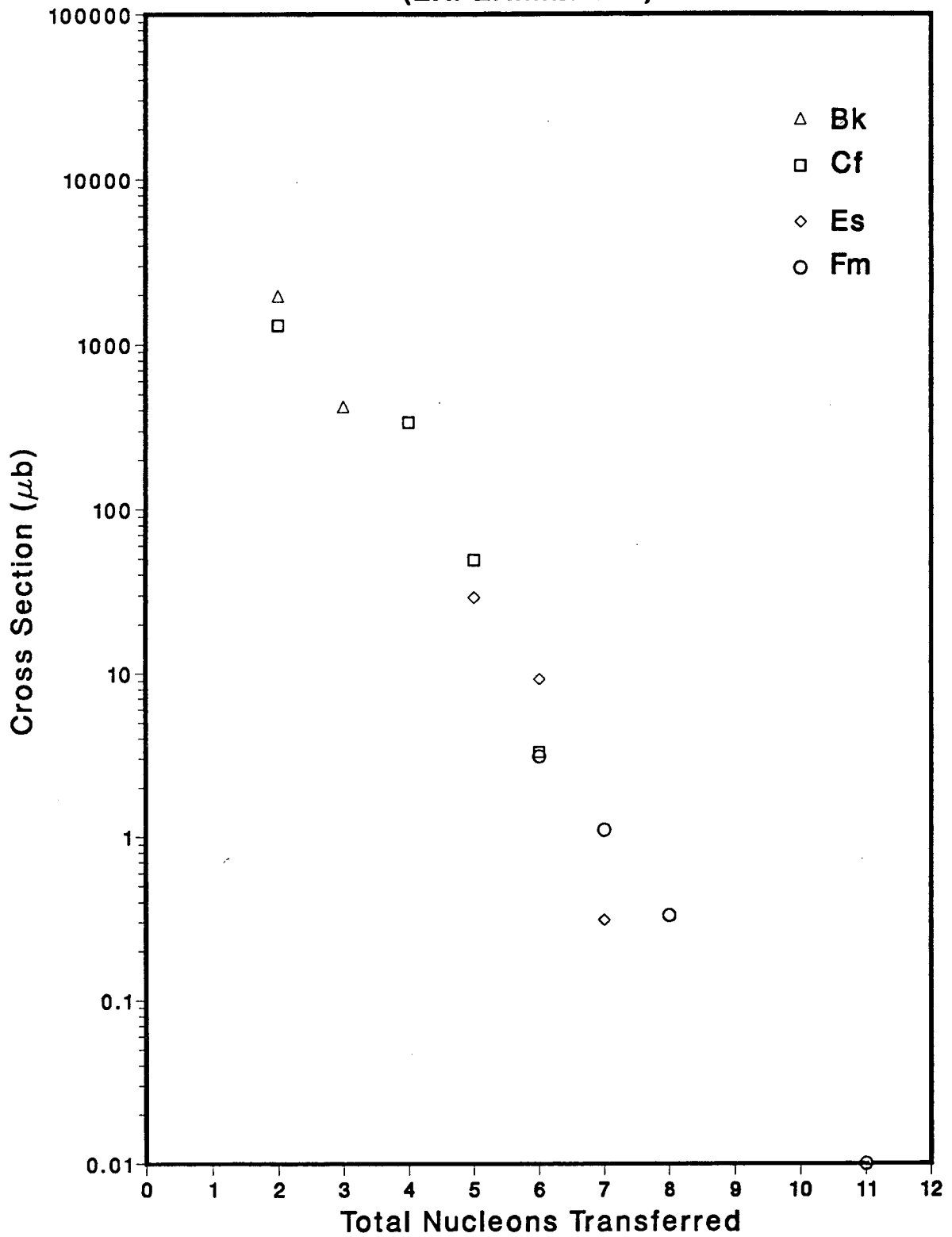


Fig. 1

$^{248}\text{Cm} + ^{16}\text{O}$
(EXPERIMENTAL)

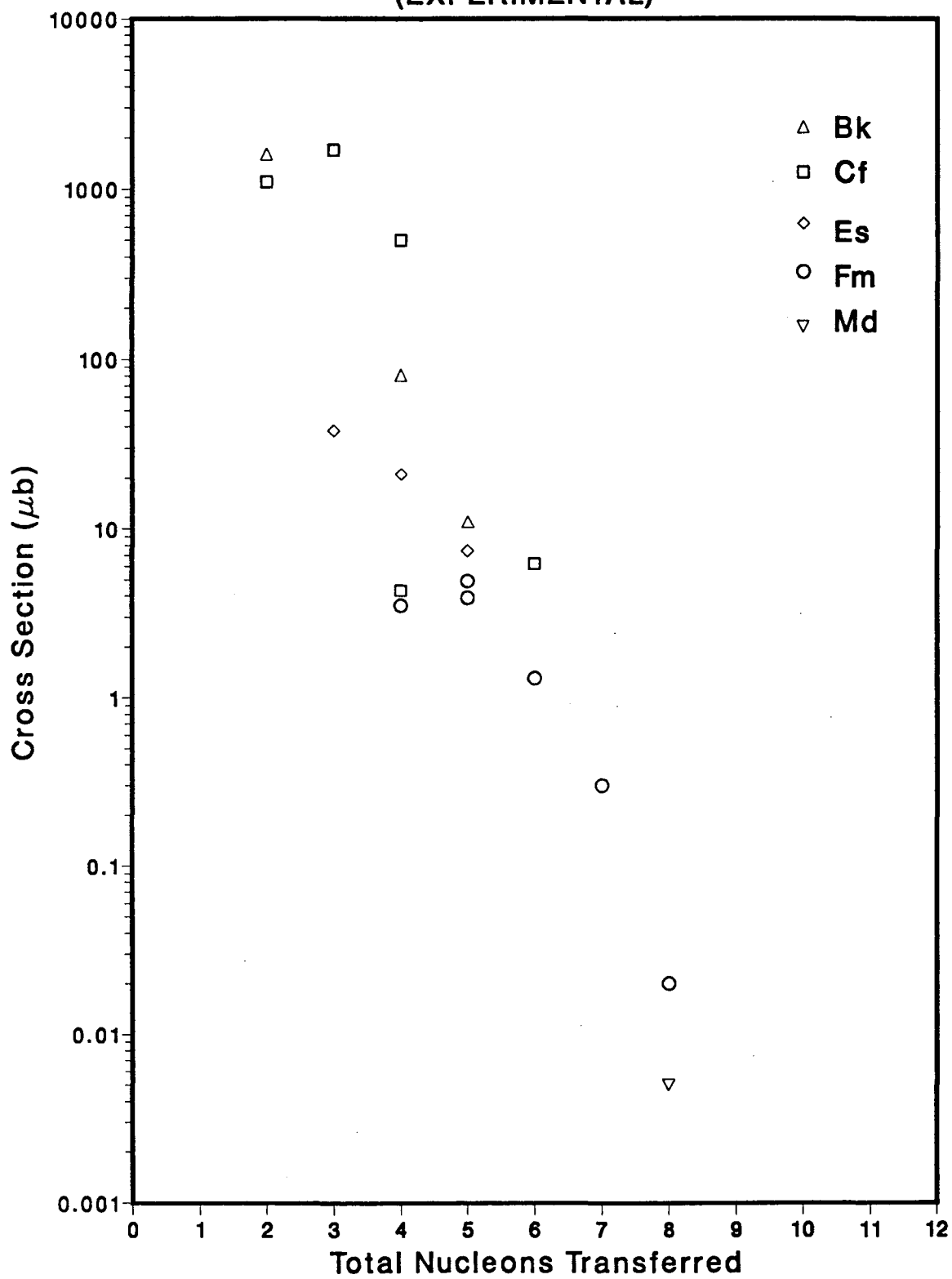


Fig. 2

$^{248}\text{Cm} + ^{18}\text{O}$
(Corrected Experimental)

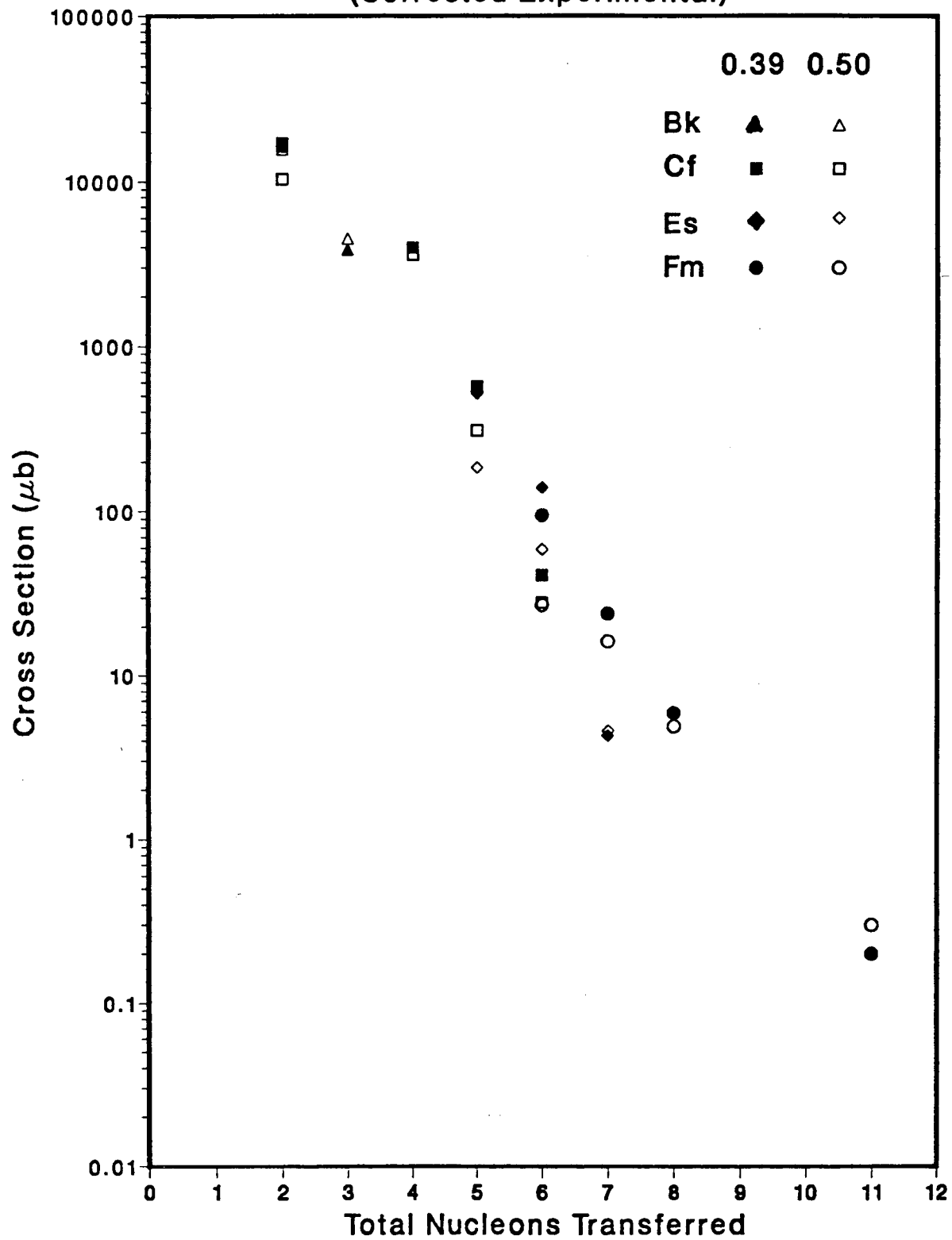


Fig. 3 (a)

$^{248}\text{Cm} + ^{18}\text{O}$

(Corrected Experimental)

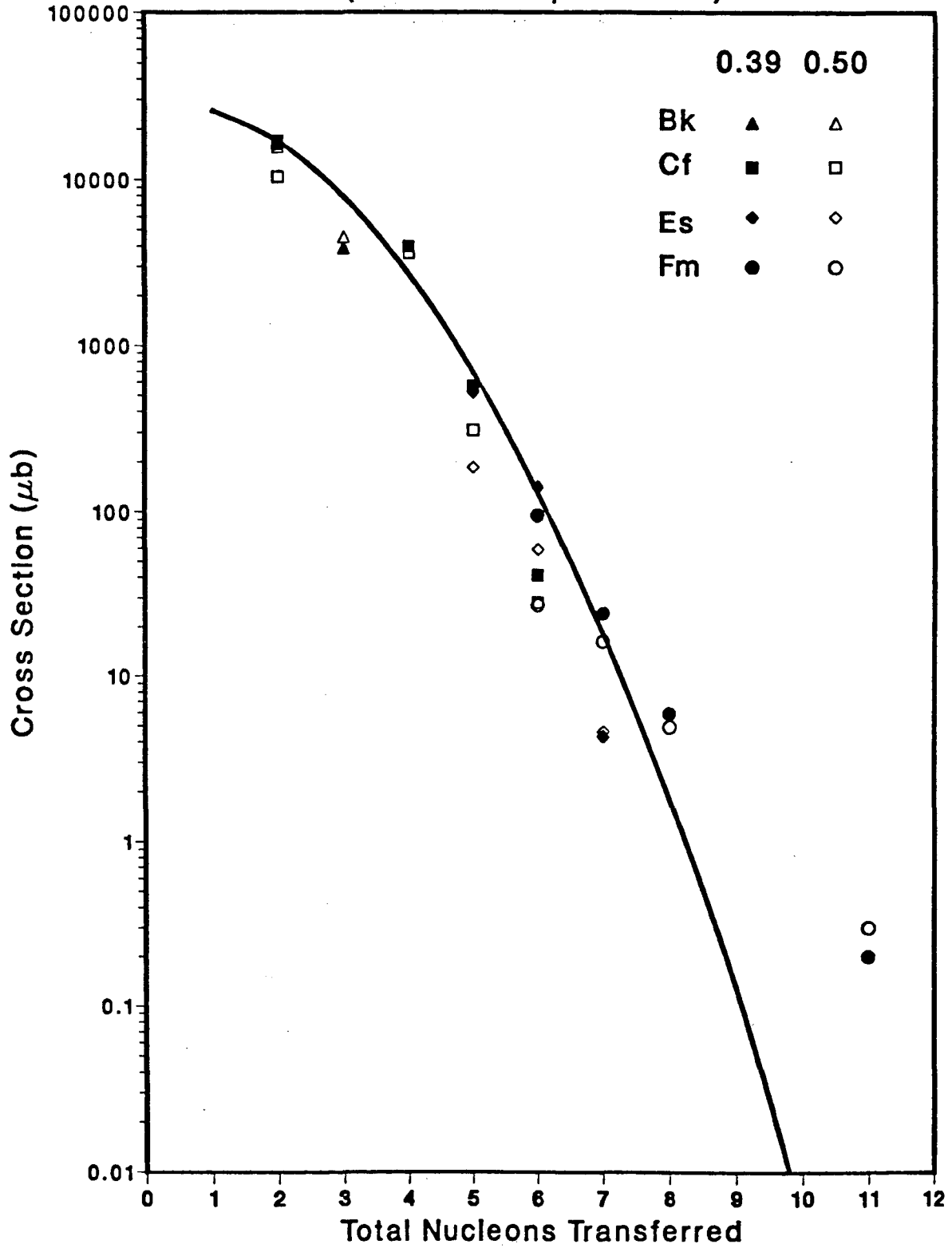


Fig. 3 (b)

$^{248}\text{Cm} + ^{16}\text{O}$
(Corrected Experimental)

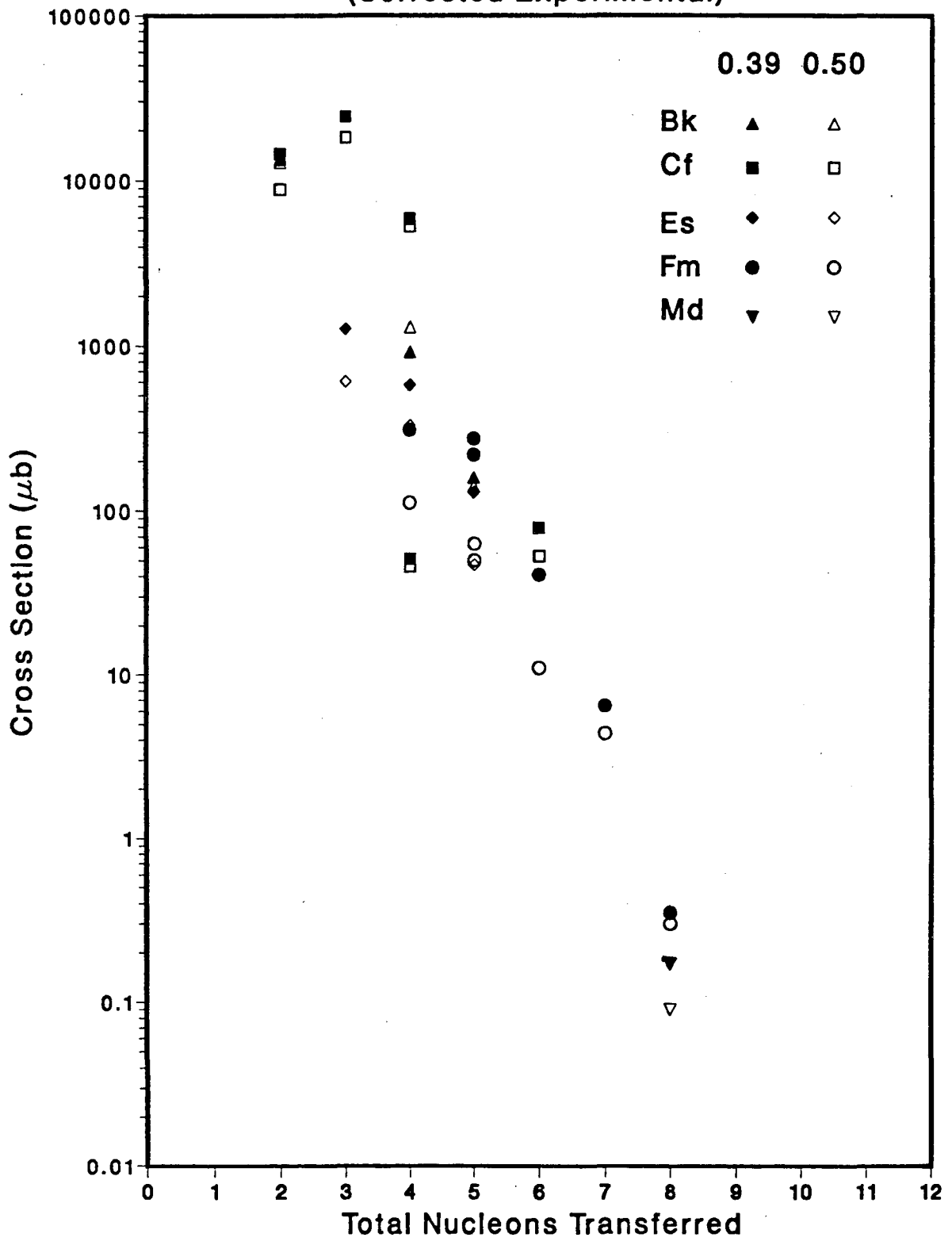


Fig. 4 (a)

$^{248}\text{Cm} + ^{16}\text{O}$
(Corrected Experimental)

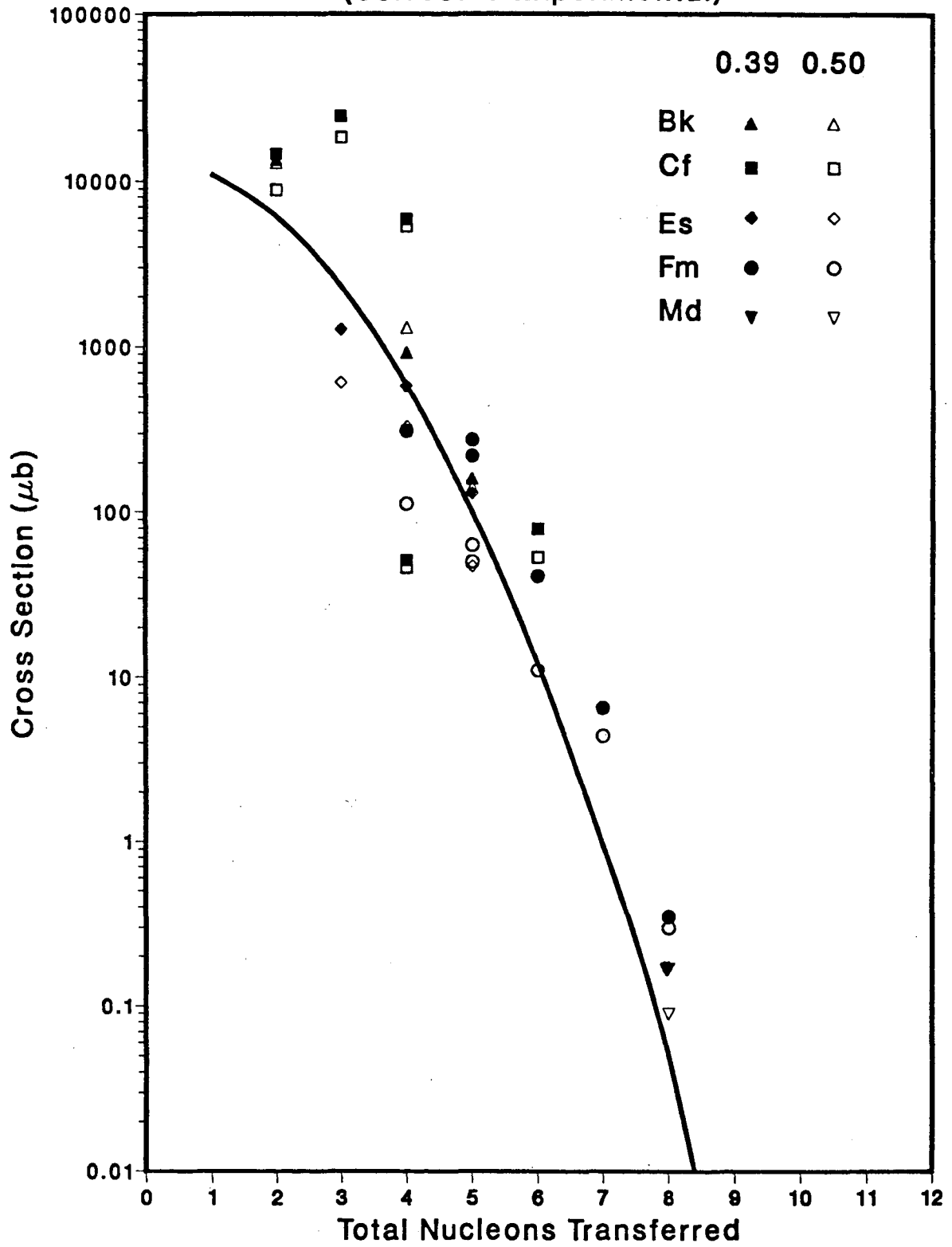


Fig. 4 (b)

$^{248}\text{Cm} + ^{18}\text{O}$
B + 1.4 MeV

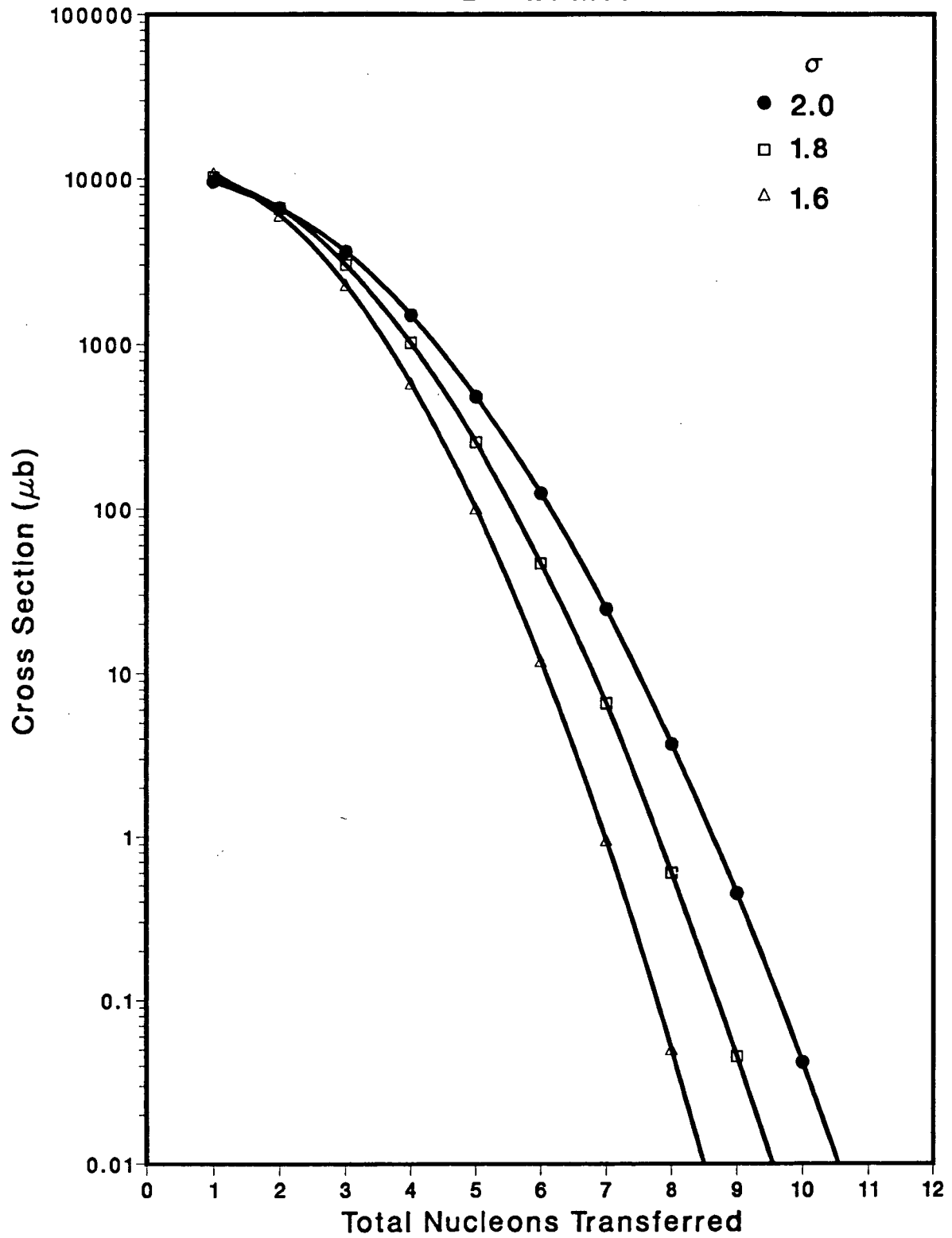


Fig. 5

$^{248}\text{Cm} + ^{16}\text{O}$
 $B + 1.4 \text{ MeV}$

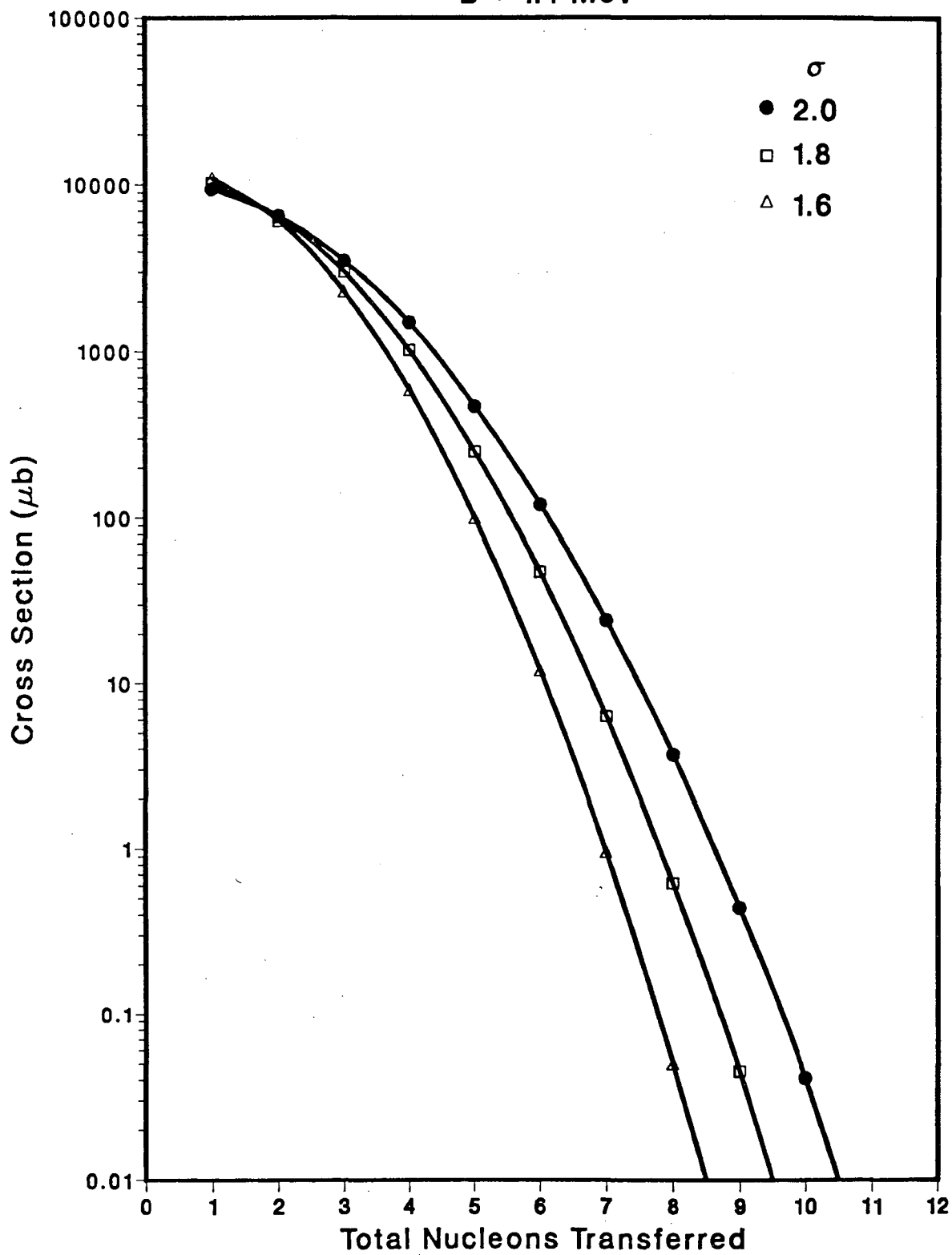


Fig. 6

$^{248}\text{Cm} + ^{18}\text{O}$
 $\sigma = 1.8$

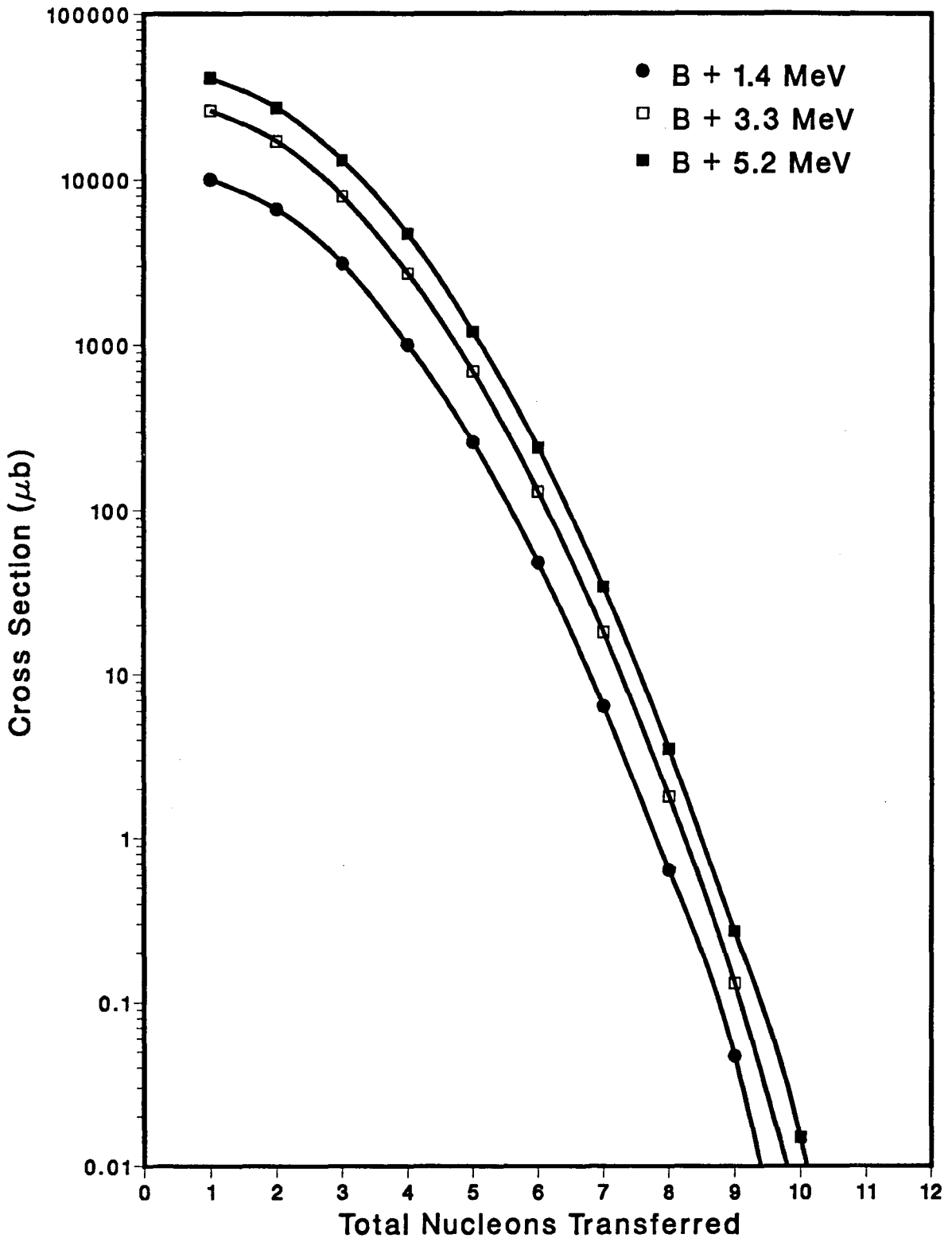


Fig. 7

$^{248}\text{Cm} + ^{16}\text{O}$

$\sigma = 1.6$

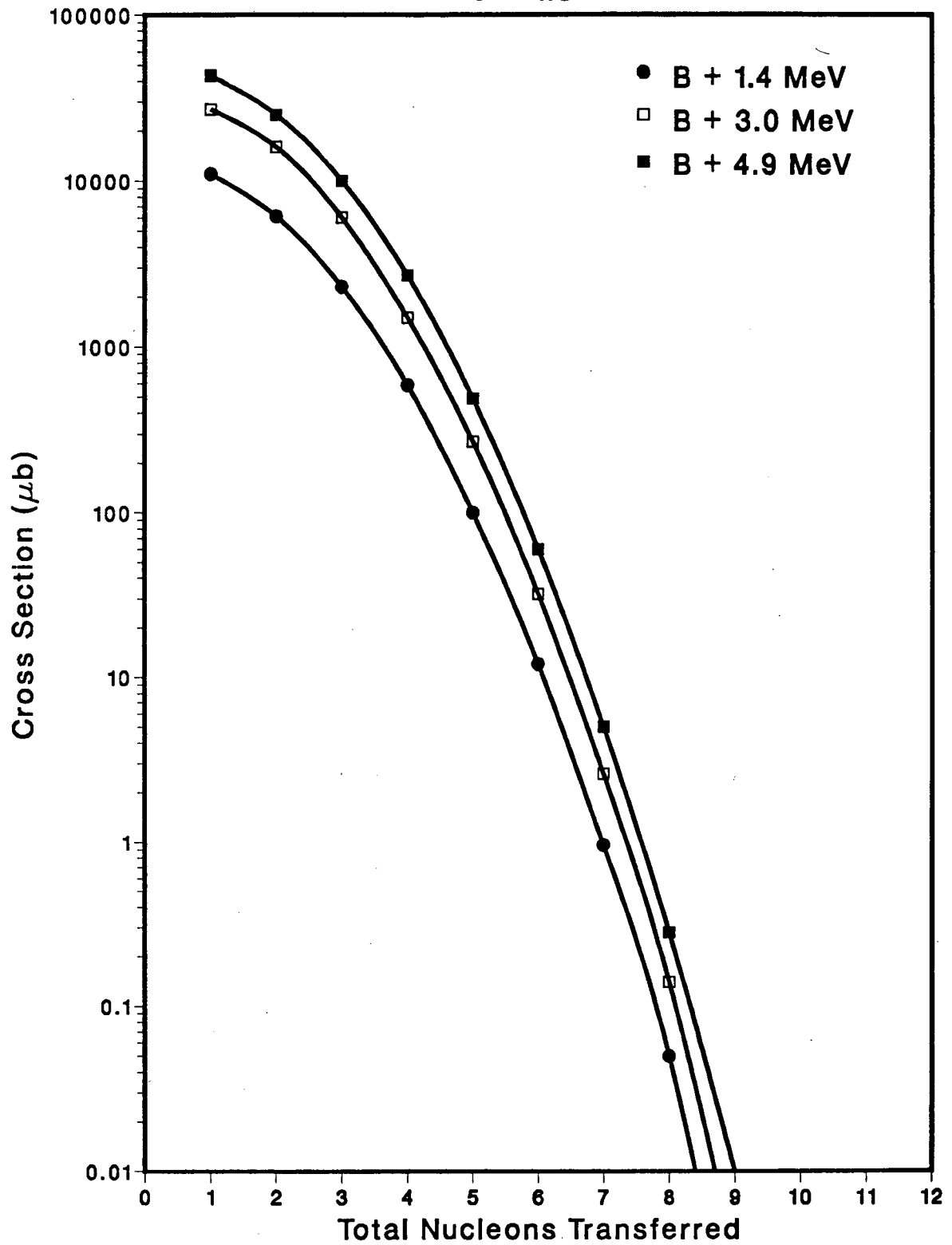


Fig. 8

$^{254}\text{Es} + ^{18}\text{O}$
(Corrected Experimental)

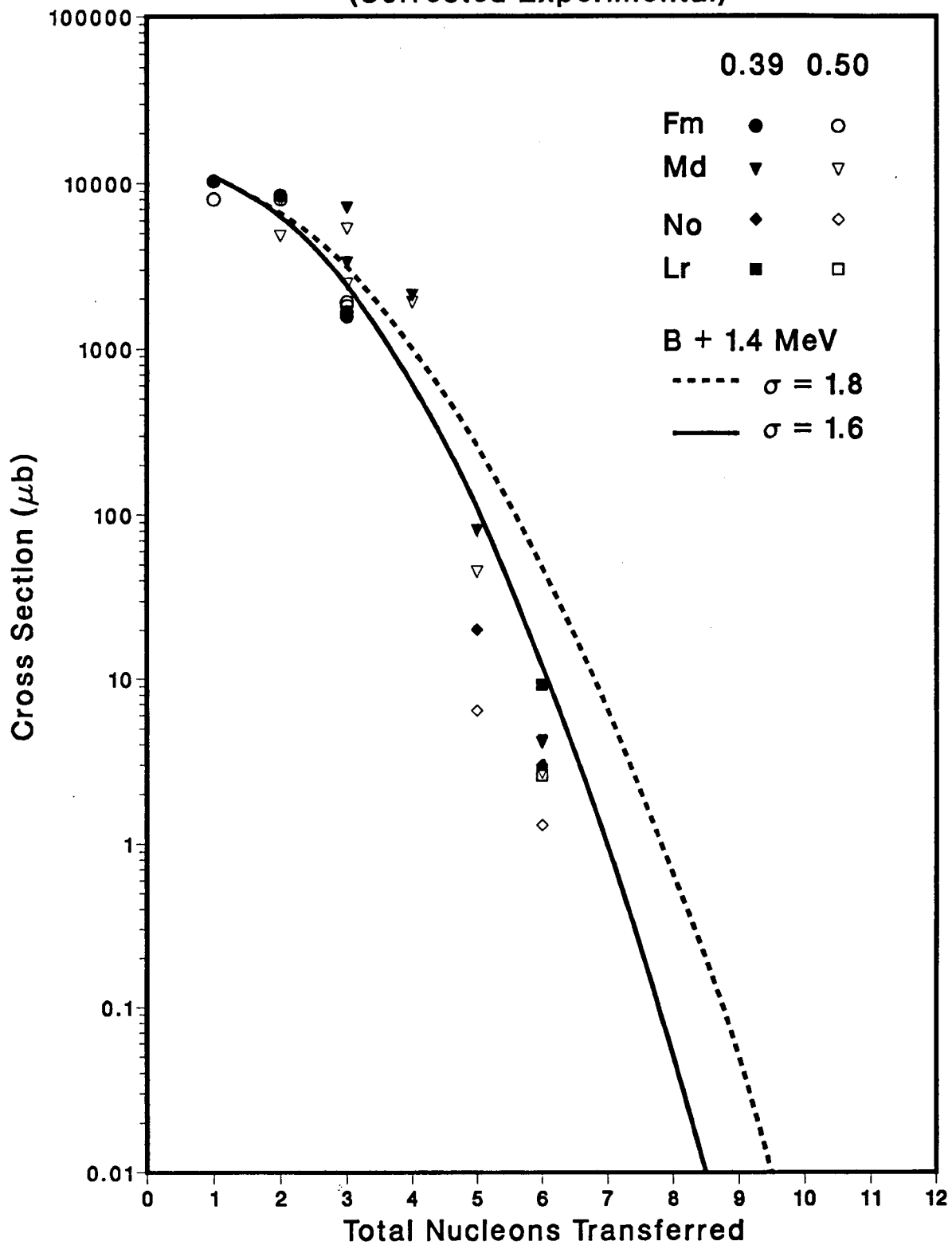


Fig. 9

APPENDIX A. PRINCIPAL EQUATIONS USED IN PWAVED5 CALCULATION

This version of the cross section calculation is labeled PWAVED5.BAS. The program first loads constants and parameters, then derived variables are calculated. No attempt was made to hold to one system of units throughout the problem; whichever units were most convenient were used. Most of the equations used in the problem are listed below. Some are accompanied by discussion or explanation.

Eq. (1): $R=1.41E-13(A)^{1/3}$ is the expression used for all nuclear radii.

Eq. (2): $MU=A(MP)(A1)(A2)/(A1+A2)$, where MP, the proton mass, is used in calculating all reduced-mass values.

Eq. (3): $RR12=R12-FF(R1)$ defines the critical distance between the centers of two nuclei. The sum of the two radii is $R1+R2=R12$ and FF is a number between 0 and 1 which defines the nuclear overlap in terms of the projectile radius, R1. RR12 is assumed to approximate the saddle point radius for $pp = 0.6$.

Eq. (4): $LMDA=h/(2ME)^{1/2}$ defines the particle wavelength.

Eq. (5): $EBV=Z1*Z2*e^2/(1.6022E-6)*R12$ represents the Coulomb barrier potential in MeV; e is in esu.

Eq. (6): $L^2=(sc)^2(2ME)$ is the angular momentum squared of the projectile-target system. In units of $h/2\pi$, the angular momentum is $SC(2ME)^{1/2}/HBAR$.

Eq. (7): $EPS=(1+(2E(SC)/Z1Z2e^2)^2)^{1/2}$ is the eccentricity term in the orbit equation.

Eq. (8): $KKK=(-m*Z1*Z2*e^2/L^2)$ represents the force term in the orbit equation.

Eq. (9): $(1/r)=(-m*Z1*Z2*e^2/L^2)*(1+(eps)*cos(theta))$. This equation for the trajectory of the scattered particle is a special solution of the general central force problem. Two coordinates are sufficient to define the motion about a central force. When the force is proportional to $(1/r)^2$, the trajectory, given by eq. (9), will be one of the conic sections and if the coordinate system is correctly chosen, the system will have rotational symmetry about the axis through the foci of the conic section. For this problem the system energy is always greater than zero, so epsilon (Eq.7) is greater than 1 and the trajectories are hyperbolic. The coordinate system is selected such that the two foci lie on the X axis with the exterior focus at the origin. Asymptotes of the hyperbola, given by $y=bx/a$ will intersect on the X axis and the angle formed by the asymptotes will be the

supplement of the scattering angle. The distance between the vertices of the two branches is $2a$ and b is the latus rectum.

Equation (9) is the same as Kepler's solution to the differential equation of motion except that the negative force term, $(-mZ_1Z_2e^2/L^2)$, defines a repulsive electrostatic force instead of the gravitational force. The value of ϵ , a constant of integration, is found by solving the elliptic integral form of the motion equation. The elliptic integral equation defines the orbit in terms of the system energy and angular momentum but is independent of time.

It is necessary that the coordinate (r) always be positive so $\cos(\theta)$ must be negative and θ must lie between $\pi/2$ and $3\pi/2$. In this coordinate system the hyperbolic trajectory intersects the X axis at the vertex of that branch of the hyperbola. In this position the radius vector (R) lies along the X axis from the focus of the exterior branch to the vertex of the orbit branch. The θ coordinate is measured from the negative X axis to the radius vector so $\theta = \pi$ at this point in the orbit.

The orbit equation is used to calculate the distance of closest approach between of the scattered particle and the scattering center. This occurs when the $\cos(\theta) = -1$ so that $(1/r) = -KKK*(1-\epsilon)$.

Eq.(10): $RMI = 1/(KKK*(\epsilon - 1))$ gives the distance between projectile and target at the point of closet approach. The trajectory for which $RMI = R_1 + R_2$ is the grazing trajectory. This trajectory also corresponds to the grazing angle of scattering and to L_{MAX} , the maximum angular momentum of the system in which nucleons can be exchanged. The critical trajectory corresponds to $RMI = R_1 + R_2 - (FF * R_1)$ and gives the critical scattering angle and the critical angular momentum.

Eq.(11): $CD = RR_{12} - RMI$. The parameter $CD = 0$ for the critical trajectory. when $CD < 0$, binary reactions occur. If $CD > 0$ the two nuclei are assumed to coalesce beyond the saddle point and fusion occurs.

Eq.(12): $RD = RR_{12} - RMI$. For the grazing trajectory, $RD = 0$. If $RD < 0$ the nuclei do not make contact. If $RD > 0$ the two nuclei come into contact and may exchange nucleons.

Eq.(13): $SCF = SCA - SCAP$. SCA is the area inside a circle of radius SC , the impact parameter for each iteration, and $SCAP$ is the area for the previous iteration. Thus, SCF is the incremental area corresponding to each single iteration and $SCFF$ is the sum of SCF for all increments. It represents the geometric cross section.

Eq. (14): $VOL = (\pi/3) * (RMI - R2)^2 * (3 - (RMI - R2))$. It is assumed that when the projectile and target nuclei are forced together in the scattering process, the smaller, more rigid projectile will distort the less rigid target and protrude into the distorted nucleus. The distance which the projectile extends into the target nucleus, to the first approximation, is $(\pi/3)h^2(3r-h)$ where $h = R1 + R2 - RMI$ and $r = ((R1)^2 + (RMI - R2)^2)^{1/2}$. The higher order terms omitted in this equation account for the change in radius of the target nucleus when it is in contact with the projectile.

Eq. (15): $VOLN = VOL * (3A1/4\pi(R1)^3)$ represents the overlap volume divided by the volume of one nucleon so it gives the overlap volume in terms of nucleons. $A1$ is the atomic number and $R1$ the radius of the projectile nucleus.

Eq. (16): $PP(q) = (1/SIG * (2\pi)^{1/2}) * \exp(-1/2 * ((q - VOLN) / (SIG))^2)$. This is the equation for the Gaussian distribution about a mean value of $VOLN$. In this calculation this expression is used to give the probability of observing (q) nucleons transferred between projectile and target assuming the mean value of (q) is $VOLN$.

Eq. (17): $PPP(q) = PP(q) * SCF$ multiplies the normalized Gaussian probability distribution, $PP(q)$, by the geometric cross section, SCF , for each iteration of the problem. The value of the Gaussian now corresponds to the geometric cross section and $PPP(q)$ to the cross section for q nucleons being transferred. $PPP(q)$ is summed over all iterations to give $PPS(q)$, the geometric cross section for the transfer of q nucleons.

Values for the scattering angles of projectile and target nuclei in the center of mass and laboratory systems are based entirely on electrostatic scattering forces using equations from Goldstein¹⁰, Chapter 3.

In the equations above, * signifies multiplication.

APPENDIX B. LIST OF VARIABLES AND CONSTANTS

VARIABLES USED IN THE PWAVED2 PROGRAM

A1,A2,A3,A4	Mass number of projectile, target, projectile-like fragment and target-like fragment, respectively
A13,A23,A33, A43	Cube root of A1, A2, A3, A4, respectively
ANG	Angle defining the overlap between target and projectile nuclei.
AREA	Area of the overlap region.
C	Velocity of light, (2.9979E+10 cm/s)
CANG	Critical scattering angle, projectile in CM system
CLAB	Critical scattering angle, projectile in laboratory system
CD	RR12-RM1, difference of critical radius and distance of closest approach
CNVE	Ergs per MeV
CNVJ	Joules per MeV
DEGG	180/pi
DF	Incremental change applied to F
E	Electronic charge, (4.8029E-10 esu)
EBV	Electrostatic potential barrier between projectile and target
ECME	Projectile energy in ergs in the center-of-mass system
ECMV	Projectile energy in MeV in the center-of-mass system
EDV	Projectile energy above the Coulomb barrier, (ECMV-EBV)
EE	Projectile energy in ergs in the laboratory system
EV	Projectile energy in MeV in the laboratory system
EPS	Trajectory parameter= $\text{SQRT}(1+((2*ECME*SC)/(Z1*Z2*E*E))^2)$
EPSL	$(4\pi\epsilon_0)^{-1}$ (mks system)
F	Fraction of R12 equal to the impact parameter,(SC)
FF	Grazing radius minus the critical radius as a function of R1, (FF*R1=R12-RR12)
H	Planck's constant (6.6262E-27 erg-sec)
HBAR	Planck's constant over 2 pi, 1.0546E-27
KKK	$(MU*Z1*Z2*E*E/SC*SC*2*M1*EE)$, a trajectory parameter
L	Angular momentum in units of h (erg-sec)
LH	Angular momentum, cgs units
LL	Angular momentum squared
LLL	$(2*L+1)$
LMDA	Equivalent wavelength of particle (Planck/momentum)
LW(I)	Angular momentum, from LCRT to LMAX
LWH(I)	Angular momentum, from LCRT to LMAX in cgs units
M1,M2,M3,M4	A1*MP, A2*MP, A3*MP, A4*MP, respectively
MP	Proton mass, (1.67265E-24 g)
MU	Reduced mass of the projectile-target system
PI	3.1415926
PP(q)	Probability for transfer of "q" nucleons according to a Gaussian distribution
PPP(q)	PP(q)*SCF(area)=cross section for the Qth iteration
PPS(q)	Sum over "q" of PPP(q)
PPD(q)	PPS(q) corrected for the multiplicity factor
PPF(q)	Cross section versus number of nucleons transferred (q)
PW(i)	Lambda squared over 4 pi multiplied by (2L+1)
R0	1.41E-13 cm
R1,R2,R3,R4	R0 multiplied by cube root of A1, A2, A3, A4, respectively

R12	$R1+R2$, radius of projectile plus radius of target nuclei
RR12	$R12-(FF*R1)$ = critical radius, inside of which fission occurs, minus a fraction (FF) of projectile radius
RD	$R12-RMI$
RMI	Distance of closest approach for projectile and target for each Rutherford trajectory
SC	Impact parameter, $(F*R12)$
SCC	Impact parameter for the critical trajectory
SCG	Impact parameter for the grazing trajectory
SCGA	Area in the circle with a radius of SCG
SCP	Impact parameter for the previous iteration
SCA	Area inside a circle with radius equal to the impact parameter, $\pi*SC^2$
SCAP	Area for the previous iteration
SCF	$(SCA-SCAP)$ = area of annulus for one iteration
SANG	Scattering angle of projectile in CM system
SLAB	Scattering angle of projectile in the laboratory system
SIGG	Sigma used in the Gaussian distribution
SCLW(I)	Impact parameter corresponding to an angular momentum of $LWH(I)$
SCLA(I)	Cross sectional area corresponding to the impact parameter $SCLW(I)$
SPW	Partial wave cross section, sum over L of λ squared divided by 4π multiplied by $(2L+1)$
TGTS	Scattering angle of target in CM system
TLAB	Scattering angle of target in laboratory system
TT	Transmission factor, $TT=1$ for geometric cross section
VOL	Volume of projectile-target overlap
VPN	Nuclear volume of one nucleon
VOLN	Number of nucleons in the overlap volume
Z1,Z2,Z3,Z4	Atomic number of the projectile, target, projectile-like fragment, and target-like fragment, respectively
NPRT	Decision flag, if $npert=1$, omit lprint of transfer cross section values except for the final iteration
VVV	Decision flag, if $VVV=1$, omit the multiplicity factor
XX	Decision flag, if $XX=1$, find the grazing trajectory
XXX	Decision flag, if $XXX=1$, omit the line print
YY	Decision flag, if $YY=1$, find the critical trajectory
ZZ	Decision flag, if $ZZ=1$, calculate the partial wave cross section

"Trajectory" means Rutherford trajectory. All scattering angles are for Rutherford scattering.

Critical values correspond to the trajectory with a distance of closest approach which simulates the fission saddle point.

If RMI is less than RR12, (R critical), fission is assumed. If RMI is greater than RR12 and less than R12 nucleon, transfers occur. If RMI is greater than R12 no interaction occurs.

Values used for Physical Constants

CNVJ=1.602192E-13 MeV per Joule

CNVE=1.602192E-6 MeV per erg

EPSL=8.991809E+9 m per Farad, 1/4pi epsilon for MKS system

PI=3.14159

C=2.99793E+10 cm/s

h=6.62617E-27 erg.s

MP=1.6726E-24 grams

E=4.8029E-10 statcoulombs/e

APPENDIX C. LISTING FOR PWAVED5 PROGRAM.

```

10 REM "THIS PROGRAM IS CALLED --PWAVED5. SIGG in line 1310..ZZ
    in line 50..
12 REM "This prgm computes the transfer of 1 to 12 nucleons using
    a Gaussian. If NPRT=0 all iterations are lprinted, NPRT=1
    lprints only final iteration.
15 DIM PP(15),PPP(15),PPS(15),PPD(15),PPF(15),IDV(15)
20 DIM LW(100),LWH(100),SCLW(100),SCLA(100),PW(100)
30 SCP=0:SCFF=0
35 XX=1:XXX=1:YY=1:VVV=1
50 ZZ=1:NPRT=1
100 EV=96
101 SC=1E-16:F=.005:FF=.6:DF=.001
105 R0=1.41E-13
110 A1=16:A2=248:A3=16:A4=248
115 Z1=8:Z2=96:Z3=8:Z4=96
130 CNVJ=1.602192E-13:CNVE=1.602192E-06:EPSL=8.991809E+09:
    PI=3.14159
140 C=2.99793E+10:H=6.63E-27:MP=1.6605E-24:E=4.8029E-10
142 DEGG=180/PI
144 A13=EXP((1/3)*LOG(A1)):A23=EXP((1/3)*LOG(A2)):
    A33=EXP((1/3)*LOG(A3)):A43=EXP((1/3)*LOG(A4))
145 M1=A1*MP:M2=A2*MP:M3=A3*MP:M4=A4*MP
150 EE=EV*CNVE
155 ECMV=EV*(A2/(A1+A2))
158 SCP=SC
160 ECME=EE*(A2/(A1+A2))
161 DF=.01
162 R1=R0*A13:R2=R0*A23:R12=R1+R2
163 RR12=R12-(FF*R1)
164 MU=MP*((A1*A2)/(A1+A2))
165 SC=F*R12
170 LMDA=H/(SQR(2*M1*EE))
175 EBV=Z1*Z2*E*E/((R12)*CNVE)
176 IF EBV>ECMV THEN GOTO 2310
178 LL=(1E+30)*SC2*(2*M1*EE)
180 LH=SQR(LL)/1E+15:L=LH/H:LLL=1+(2*L)
190 EPS#=SQR(1#+((2*EE*SC)/(Z1*Z2*E*E))2)
195 KKK=(1E+30)*(MU*Z1*Z2*E*E)/LL
200 RMI=1/(KKK*(EPS#-1))
201 IF RMI>R12 THEN GOTO 1205
202 CD=RR12-RMI
203 RD=R12-RMI
205 IF XX=1 THEN GOTO 2222
208 IF YY=1 THEN GOTO 2444
209 IF ZZ=1 THEN GOTO 1500
210 SCA=PI*SC2
220 SCAP=PI*SCP2
230 SCF=SCA-SCAP
235 SCFF=SCFF+SCF
240 SANG=2*ATN((Z1*Z2*E*E)/(2*SC*EE))

```

```

245 SLAB=ATN((SIN(SANG))/(COS(SANG)+(M1/M2)))
247 IF SLAB<0 THEN SLAB=SLAB+PI
250 TGTS=(SANG-PI)
  255 TLAB=ATN((SIN(TGTS))/(COS(TGTS)+1))
  256 SANG=DEGG*SANG:SLAB=DEGG*SLAB:TGTS=DEGG*TGTS:TLAB=DEGG*TLAB
  260 IF XXX=1 THEN GOTO 1000
  262 PRINT:PRINT "SANG="SANG,"SLAB="SLAB,"TGTS="TGTS,"TLAB="TLAB
  270 LPRINT:LPRINT "257","SANG="SANG,"SLAB="SLAB,"TGTS="TGTS,"
    TLAB="TLAB
  282 XXX=1
1000 REM "orbit, 1/r=- (m*z*z'*e*e/l*1)(1+eps*cosi),
    eps=sqr(1+(2Es/zz'ee)2), also, rr(mzz'ee/ll)eps*sini=0 for
    closest approach."
1005 IF RMI<RR12 GOTO 1055
1015 IF RMI>R12 THEN 1205 ELSE 1100
1055 F=F+.01
1060 GOTO 105
1100 REM "Calculate the projected area of nuclear overlap"
1110 ANG=ATN((SQR(R22-(RMI-R2)2))/(RMI-R2))
1120 AREA=1E+30*((PI*R12)*(ANG/2*PI))-(RMI-R2)*
    SQR(R12-(RMI-R2)2)
1130 VOL=1E+26*(PI/3)*((1E+10)*(2*R13)+(1E+10)*((RMI-R2)3-
    (3E+10)*R12*(RMI-R2))
1140 VPN=9.999999E+35*(4*PI*R13)/(3*A1)
1150 VOLN=VOL/VPN
1160 IF NPRT=1 THEN 1230 ELSE 1210
1205 IF NPRT=1 THEN 1210 ELSE 1400
1210 LPRINT:LPRINT "RR/SC/VOLN/LCT RMI/SA/-/L R12/SF/-/LMX
    GAG/SAG/CAG/TGS GLB/SLB/CLB/TLB"
1220 LPRINT RR12,RMI,R12,GANG,GLAB,SC,SCA,SCF,SANG,SLAB,VOLN,,,
    CANG,CLAB,LCRT,L,LMAX,TGTS,TLAB
1225 IF NPRT=1 GOTO 1260
1230 PRINT:PRINT "RR/SC/VOLN/LCT RMI/SA/-/L R12/SF/-/LMX
    GAG/SAG/CAG/TGS GLB/SLB/CLB/TLB"
1240 PRINT RR12,RMI,R12,GANG,GLAB,SC,SCA,SCF,SANG,SLAB,VOLN,,,
    CANG,CLAB,LCRT,L,LMAX,TGTS,TLAB
1245 PRINT "SCF="SCF,"SCFF="SCFF:PRINT
1250 PRINT "PROB,n=1 to 12 Prob*area(SC) SUM PROB /exit chann
    trnsm"
1252 PRINT " PP(q) PPP(q) PPS(q) PPD(q)
    PPF(q) "
1255 IF NPRT=1 GOTO 1305
1260 LPRINT "SCF="SCF,"SCFF="SCFF:LPRINT:LPRINT "PROB,n=1 to 12
    Prob*area(SC) SUM PROB /exit chann trnsm factor"
1262 LPRINT" PP(q) PPP(q) PPS(q) PPD(q)
    PPF(q) "
1265 IF NPRT=1 GOTO 1370
1305 FOR Q=1 TO 12
1310 SIGG=1.8
1315 PP(Q)=(1/(SIGG*SQR(2*PI)))*(EXP((-1/2)*((Q-VOLN)/SIGG)2))
1320 PPP(Q)=PP(Q)*SCF
1325 PPS(Q)=PPS(Q)+PPP(Q)

```

```

1330 PPD(Q)=PPS(Q)*1
1331 IF VVV=1 THEN 1335
1332 PPD(Q)=PPS(Q)*(1/(4*Q))
1335 TT=1
1340 PPF(Q)=PPD(Q)*TT
1345 NEXT Q
1350 FOR Q=1 TO 12
1355 PRINT PP(Q),PPP(Q),PPS(Q),PPD(Q),PPF(Q)
1360 NEXT Q
1365 IF NPRT=1 GOTO 1390
1370 FOR Q=1 TO 12
1375 LPRINT PP(Q),PPP(Q),PPS(Q),PPD(Q),PPF(Q)
1377 NEXT Q
1380 IF NPRT=1 GOTO 1400
1390 F=F+.02
1395 GOTO 105
1400 PRINT "RMI>R12", "EV="EV, "ECMV="ECMV, "EBV="EBV, "R0="R0,
      "SIGG="SIGG
1405 LPRINT "RMI>R12", "EV="EV, "ECMV="ECMV, "EBV="EBV, :LPRINT
      "R0="R0, "SIGG="SIGG
1410 STOP
1420 GOTO 101
1500 REM "1500 to 1600 is partial wave summ..
1510 SPW=0
1515 PRINT:PRINT "LMDA="LMDA:PRINT " Lw", " SCLw", " Pw", "
      sumPw", " SCLA"
1518 LPRINT:LPRINT "EV="EV, "ECMV="ECMV, "EBV="EBV
1519 LPRINT "LMAX="LMAX, "LCRT="LCRT, "GANG="GANG, "CANG="CANG
1520 LPRINT "LMDA="LMDA:LPRINT " Lw", " SCLw", " Pw", " sumPw", "
      SCLA"
1530 FOR I=INT(LCRT) TO INT(LMAX)
1535 LW(I)=I:LWH(I)=LW(I)*HBAR
1540 SCLW(I)=LWH(I)/SQR(2*M1*EE)
1545 SCLA(I)=SCLW(I)^2*PI
1550 PW(I)=((LMDA^2)/(4*PI))*((2*LW(I))+1)
1560 SPW=SPW+PW(I)
1570 PRINT LW(I), SCLW(I), PW(I), SPW, SCLA(I)
1575 LPRINT LW(I), SCLW(I), PW(I), SPW, SCLA(I)
1580 NEXT I
1590 STOP
1595 ZZ=0: GOTO 210
2202 SCG=SC:SCGA=PI*(SCG)^2
2204 LMAX=(SCG*SQR(2*M1*EE))/HBAR
2205 GANG=2*ATN((Z1*Z2*E*E)/(2*SCG*EE))
2206 GLAB=ATN((SIN(GANG))/(COS(GANG)+(M1/M2))):GANG=DEGG*GANG:
      GLAB=DEGG*GLAB
2208 PRINT "2208", "Z1,2,3,4="Z1 Z2 Z3 Z4, "A1,2,3,4="A1 A2 A3 A4,
      "EV="EV, "ECMV="ECMV, " EBV="EBV, "LMAX="LMAX, " GANG="GANG, "
      SCG="SCG, "SCGA="SCGA
2209 LPRINT:LPRINT "2209", "Z1,2,3,4="Z1 Z2 Z3 Z4, "A1,2,3,4="A1 A2
      A3 A4, "EV="EV, "ECMV="ECMV, " EBV="EBV, "LMAX="LMAX, " GANG=
      "GANG, " SCG="SCG, "SCGA="SCGA

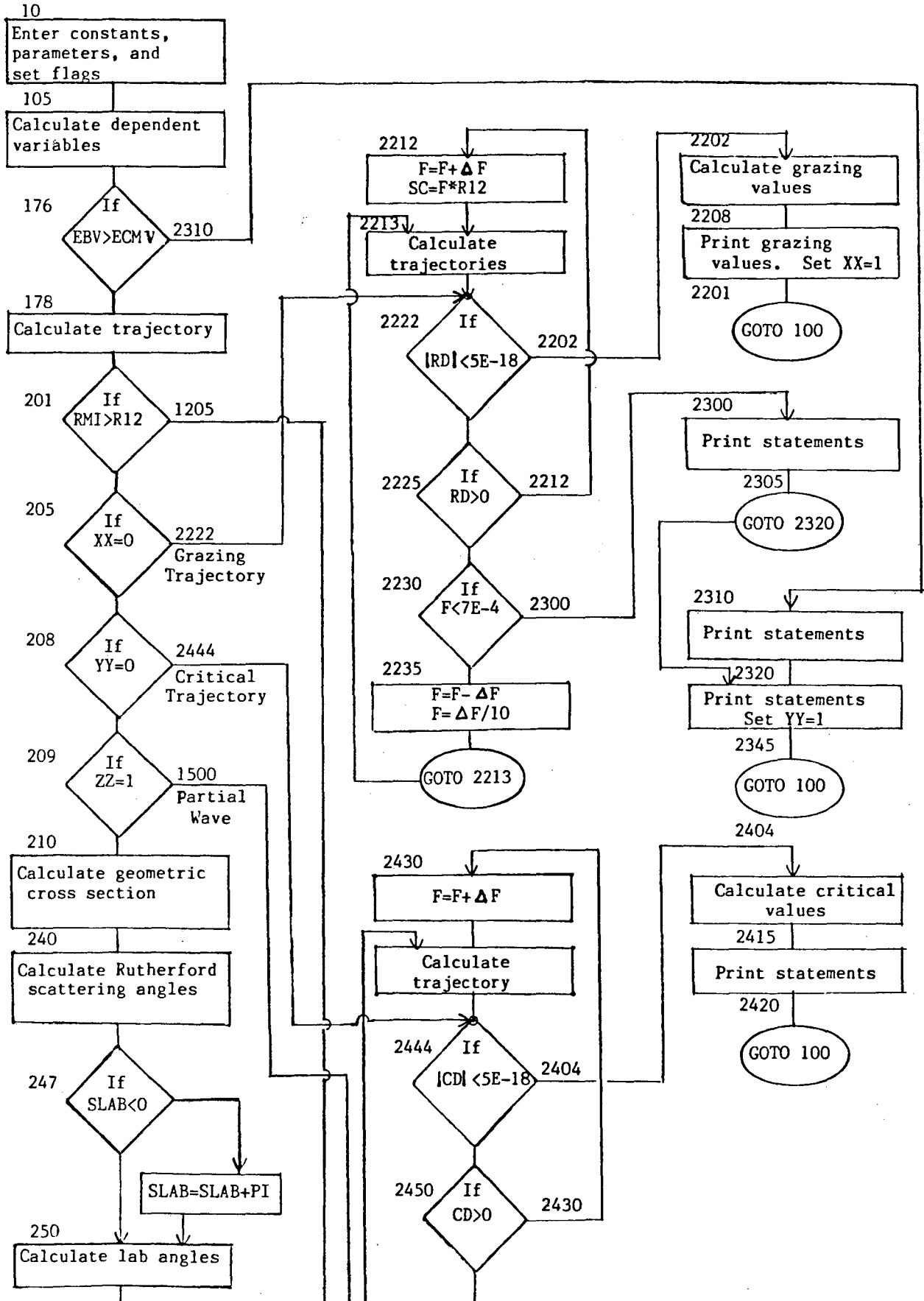
```

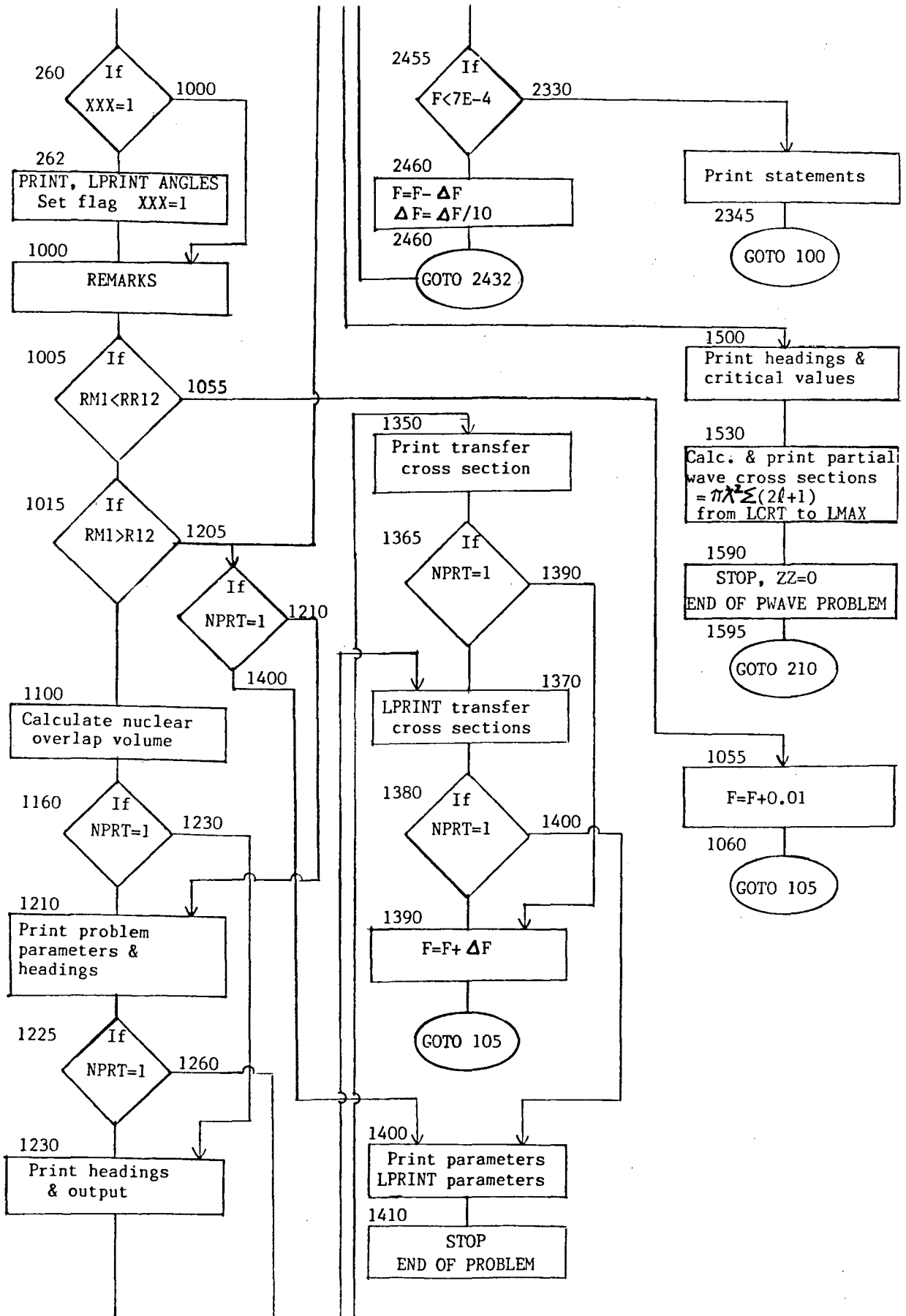
```

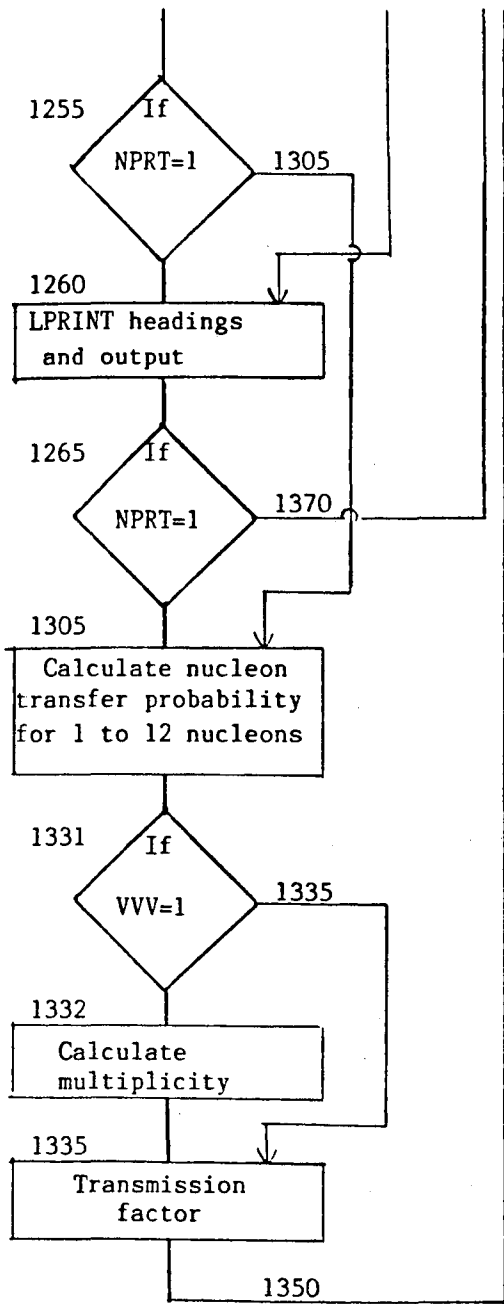
2210 XX=0:GOTO 100
2212 F=F+DF
2213 SC=F*R12
2214 L=(SC*SQR(2*M1*EE))/H
2216 EPS#=SQR(1#+((2*EE*SC)/(Z1*Z2*E*E))^2)
2218 KK=(MU*Z1*Z2*E*E)/(L*H):KKK=KK/(L*H)
2219 RMI=1/(KKK*(EPS#-1)):RD=R12-RMI
2222 IF ABS(RD)<5E-18 THEN 2202
2225 IF RD>0 THEN 2212
2230 IF F<.0007 THEN 2300
2235 F=F-DF:DF=DF/10:GOTO 2213
2300 PRINT "NO INTERACTION AT THIS ENERGY! INCREASE EV TO
RETRY."
2305 PRINT "F="F,"SC="SC,"RMI="RMI,"R12="R12,"RD="RD:GOTO 2320
2310 PRINT "ECMV BELOW COULOMB BARRIER, INCREASE EV"
2320 PRINT "EV="EV,"ECMV="ECMV,"EBV="EBV:STOP:GOTO 100
2330 PRINT "CANNOT REACH CRITICAL RADIUS AT THIS ENERGY!"
2335 SCC=0:LCRT=0:CANG=0:YY=0
2340 PRINT "EV="EV,"ECMV="ECMV,"EBV="EBV,"LCRT="LCRT,"CANG="CANG,
"LMAX="LMAX,"GANG="GANG
2345 GOTO 100
2404 SCC=SC:SCCA=PI*(SCC)^2
2405 SCAA=SCGA-SCCA
2406 LCRT=(SCC*SQR(2*M1*EE))/HBAR
2408 CANG=2*ATN((Z1*Z2*E*E)/(2*SCC*EE))
2410 CLAB=ATN((SIN(CANG))/(COS(CANG)+(M1/M2))):CANG=DEGG*CANG:
CLAB=DEGG*CLAB
2413 YY=0
2415 PRINT "2415","EV="EV,"ECMV="ECMV,"EBV="EBV,"LMAX="LMAX,
"GANG="GANG,"SCG="SCG,"LCRT="LCRT,"CANG="CANG,"SCC="SCC,
"SCCA="SCCA,"SCGA-SCCA="SCAA
2417 LPRINT "2415","EV="EV,"ECMV="ECMV,"EBV="EBV,"LMAX="LMAX,
"GANG="GANG,"SCG="SCG,"LCRT="LCRT,"CANG="CANG,"SCC="SCC,
"SCCA="SCCA,"SCGA-SCCA="SCAA
2420 GOTO 100
2430 F=F+DF
2432 SC=F*R12
2434 L=(SC*SQR(2*M1*EE))/H
2436 EPS#=SQR(1#+((2*EE*SC)/(Z1*Z2*E*E))^2)
2438 KK=(MU*Z1*Z2*E*E)/(L*H):KKK=KK/(L*H)
2440 RMI=1/(KKK*(EPS#-1)):CD=RR12-RMI
2444 IF ABS(CD)<5E-18 THEN 2404
2450 IF CD>0 THEN 2430
2455 IF F<.0007 THEN 2330
2460 F=F-DF:DF=DF/10:GOTO 2432
2546 STOP

```


APPENDIX D. FLOW DIAGRAM FOR PWAVED5 CALCULATION







LAWRENCE BERKELEY LABORATORY
UNIVERSITY OF CALIFORNIA
INFORMATION RESOURCES DEPARTMENT
BERKELEY, CALIFORNIA 94720